Depolarizing surface scattering by a birefringent material with rough surface

Jonas Ritter[a,b], Ning Ma[a], Wolfgang Osten[a], Mitsuo Takeda[c], Wei Wang[a,*]

[a] *Institute of Photonics and Quantum Sciences, School of Engineering and Physical Sciences, Heriot-Watt University, Edinburgh EH14 4AS, UK*
[b] *Institute of Applied Optics, University of Stuttgart, Pfaffenwaldring 9, 70569 Stuttgart, Germany*
[c] *Center for Optical Research and Education (CORE), Utsunomiya University, Yoto 7-1-2, Utsunomiya, Tochigi 321-8585, Japan*

Abstract

The surface polarization scattering is investigated in terms of the coherence matrix for the electric field scattered from a birefringent material with a random interface between its surface and air. The relationship between the statistical properties of the scattered light at the scattering surface and the micro-structure of the anisotropic media has been explored for the first time to understand the underlying mechanism of the surface scattering phenomena for the electric field with random states of polarization.

Keywords: Scattering from surfaces, Coherence in wave optics, Statistics, Polarization in wave optics
PACS: 68.49.-h, 42.25.Kb, 02.50.-r, 42.25.Ja,

As a ubiquitous natural phenomenon, the scattering of electromagnetic waves has been studied extensively and various techniques have been developed during the last decades [1, 2, 3, 4]. As the deflection of a ray from straight path, light scattering is a model of energy re-distribution where light in the form of propagating energy is scattered due to irregularities on a surface. Optical scattering is important for many applications such as detection of surface defects, determination of the contamination of optical systems, medical diagnosis or quality control of food and agricultural product. In

*Corresponding author
Email address: w.wang@hw.ac.uk (Wei Wang)

the majority of studies on the light scattering, the material surface to generate the scattering fields has been treated as rough without considering a material having an anisotropic refractive index that affects the polarization and propagation direction of the transmitted light. Nonetheless, it is still of considerable interest to understand the condition under which the statistical properties of the rough surface of the birefringent material can affect the coherence and polarization properties of the scattered electric fields. The presented research results can be regarded as the first trial in the analysis of scattering electromagnetic waves from a rough surface of birefringent material. For example, quality control of surface roughness for polarizing optical elements plays an important role in optical manufacturing engineering since it will influence polarization function, extinction ratio, laser damage resistance and wave-front distortion. Furthermore, the studies of the scattered light from rough-surfaced birefringent material have found their applications in other engineering fields including optical meteorology, biomedical imaging and bioengineering. In our previous study, the statistics of the polarization speckle generated by a retardation plate with a rough surface has been investigated [5]. This paper is an extension of our previous study through exploring how the coherence and polarization properties of the scattered light depend on the micro-structure of the rough surfaces of birefringent material, such as a quartz, a calcite and plastics et. al.

As shown in Figure 1, we assume free-space transmission geometry for surface polarization scattering, where an example of a cross-section of the birefringent material with a typical random surface height fluctuation has been given. Just as the laser speckle generated from the rough surface, the relationship between these height variations of the rough-surfaced retardation plate and the amplitude variations of the scattered electric field is in general an extremely complex one. It is influenced by variations of surface slope, shadowing of retardation plate, multiple scattering and reflection inside the birefringent material, and polarization effects introduced to the scattered wave travelling in the retardation plate in arbitrary directions with reference to as compared with the orientation of fast/slow axis of birefringent material. For purpose of analysis in this letter, we will adopt a simplified model to give some physical in-sight into the relationship between the surface height fluctuations for the rough-surfaced retardation plate and the polarization fluctuations of the scattered electric field.

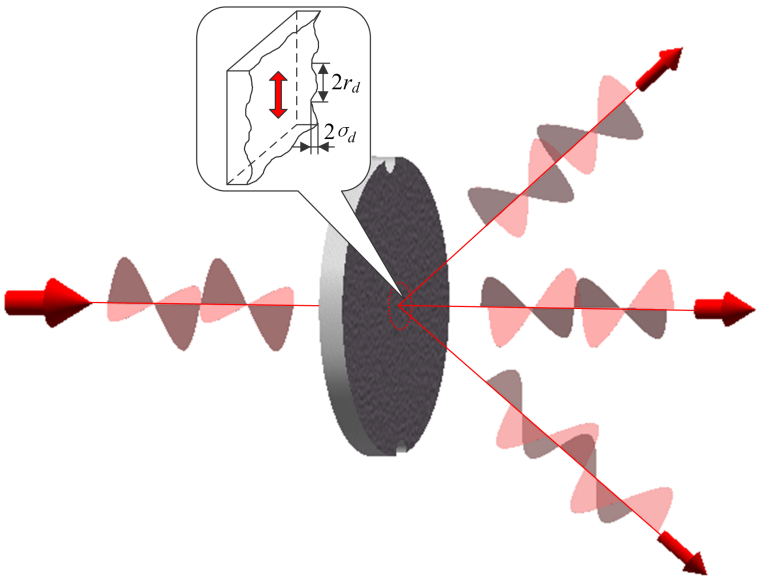

Figure 1: Schematic diagram of surface polarization scattering from a rough surface of anisotropic media with an example of a cross-section of a typical surface thickness fluctuation.

Let the scattered electric field immediately behind the rough surface, $\mathbf{E}^{\mathrm{t}}(\mathbf{r})$, be related to the incident electric vector $\mathbf{E}^{\mathrm{i}}(\mathbf{r})$ through the Jones matrix $\mathbf{T}(\mathbf{r})$ for a birefringent material with its fast/slow axis aligned along $\hat{\mathrm{y}}$ direction given by

$$\mathbf{T}(\mathbf{r}) = \begin{pmatrix} \mathrm{e}^{-\mathrm{j}\varphi_{\mathrm{x}}(\mathbf{r})} & 0 \\ 0 & \mathrm{e}^{-\mathrm{j}\varphi_{\mathrm{y}}(\mathbf{r})} \end{pmatrix}, \tag{1}$$

where $\varphi_m\,(m = \mathrm{x}, \mathrm{y})$ is the effective phase delay for the $\hat{\mathrm{x}}$ or $\hat{\mathrm{y}}$ components of the electric field introduced by an optical path passing through the retardation plate with surface height fluctuation and the remaining region of free space. Under the assumption that the coherence property of the incident illumination field and the correlation property of the depolarizer are statistically independent, we have the transmission coherence matrix $\mathbf{W}^{\mathrm{t}}(\mathbf{r}_1, \mathbf{r}_2)$ of the modulated fields just behind the depolarizer [5, 6, 7, 8]. That is

$$\mathbf{W}^{\mathrm{t}}(\mathbf{r}_1, \mathbf{r}_2) = \begin{pmatrix} W^{\mathrm{i}}_{\mathrm{xx}}(\mathbf{r}_1, \mathbf{r}_2) \left\langle \mathrm{e}^{\mathrm{j}\Delta\varphi_{\mathrm{xx}}(\mathbf{r}_1, \mathbf{r}_2)} \right\rangle & W^{\mathrm{i}}_{\mathrm{xy}}(\mathbf{r}_1, \mathbf{r}_2) \left\langle \mathrm{e}^{\mathrm{j}\Delta\varphi_{\mathrm{xy}}(\mathbf{r}_1, \mathbf{r}_2)} \right\rangle \\ W^{\mathrm{i}}_{\mathrm{yx}}(\mathbf{r}_1, \mathbf{r}_2) \left\langle \mathrm{e}^{\mathrm{j}\Delta\varphi_{\mathrm{yx}}(\mathbf{r}_1, \mathbf{r}_2)} \right\rangle & W^{\mathrm{i}}_{\mathrm{yy}}(\mathbf{r}_1, \mathbf{r}_2) \left\langle \mathrm{e}^{\mathrm{j}\Delta\varphi_{\mathrm{yy}}(\mathbf{r}_1, \mathbf{r}_2)} \right\rangle \end{pmatrix}, \tag{2}$$

where $\mathbf{W}^{\mathrm{i}}(\mathbf{r}_1, \mathbf{r}_2)$ is the coherence matrix of the incident electric fields, angu-

lar brackets $\langle ... \rangle$ denote ensemble average, $\Delta\varphi_{lm}(\mathbf{r}_1, \mathbf{r}_2) = \varphi_l(\mathbf{r}_1) - \varphi_m(\mathbf{r}_2)$, $(l, m = \mathrm{x}, \mathrm{y})$ are the difference of the effective phase delay for each components of the electric fields.

For demonstration purposes only, and without loss of generality, we assume that the incident light is a linearly polarized, spatially coherent, plane wave for which the coherence matrix is given by

$$\mathbf{W}^{\mathrm{i}}(\mathbf{r}_1, \mathbf{r}_2) = I_0 \begin{pmatrix} \cos^2\theta & \cos\theta\sin\theta \\ \cos\theta\sin\theta & \sin^2\theta \end{pmatrix}, \tag{3}$$

where I_0 is the on-axis intensity of the incident field and θ is the linear polarization angle with $\hat{\mathrm{x}}$-axis. Some further progress can be made for Eq. 2 when certain assumptions for the effective phase delay and the correlation function of the surface thickness are specified [9, 10, 11]. For simplicity, the assumption is usually made that the effective phase delays (or equivalently the surface height fluctuations) is a Gaussian random process. We have

$$\begin{aligned} \left\langle \mathrm{e}^{\mathrm{j}\Delta\varphi_{lm}} \right\rangle &= \left\langle \exp\left\{ \mathrm{j}\,(2\pi/\lambda)\left[(n_l - 1)(\overline{d} + d(\mathbf{r}_1)) - (n_m - 1) \right.\right.\right. \\ &\quad \left.\left.\left. \times(\overline{d} + d(\mathbf{r}_1)) \right] \right\} \right\rangle \\ &= \exp\left\{ (\mathrm{j}2\pi/\lambda)(n_l - n_m)\overline{d} \right\} \left\langle \exp\left\{ \mathrm{j}(2\pi/\lambda)\left[(n_l - 1) \right.\right.\right. \\ &\quad \left.\left.\left. \times d(\mathbf{r}_1) - (n_m - 1) d(\mathbf{r}_2) \right] \right\} \right\rangle \\ &= \exp\left\{ (\mathrm{j}2\pi/\lambda)(n_l - n_m)\overline{d} \right\} \exp\left\{ -(2\pi^2/\lambda^2)\left[(n_l - 1)^2 \right.\right. \\ &\quad \times < d^2(\mathbf{r}_1) > + (n_m - 1)^2 < d^2(\mathbf{r}_2) > - 2(n_l - 1)(n_m - 1) \\ &\quad \left.\left. \times < d(\mathbf{r}_1) d(\mathbf{r}_2) > \right] \right\}, \end{aligned} \tag{4}$$

where λ is the wavelength in vacuum, $d(\mathbf{r})$ is the zero mean Gaussian random thickness variation around the average thickness $\bar{d}$ of the birefringent plate, n_l and n_m are the refractive indices for the birefringent material. Another assumption is that the correlation function of the surface thickness takes also Gaussian form,

$$\langle d(\mathbf{r}_1) d(\mathbf{r}_2) \rangle = \sigma_{\mathrm{d}}^2 \exp\{ -|\mathbf{r}_1 - \mathbf{r}_2|^2 / r_{\mathrm{d}}^2 \}, \tag{5}$$

where σ_{d}^2 and r_{d} are mutually independent quantities indicating the variance of the $d(\mathbf{r})$ and the radius at which the normalized surface thickness correlation falls to 1/e, respectively. Therefore, the transmission coherence tensor of

the scattered electric field immediately behind the scattering layer becomes a complex Hermitian matrix.

$$W^{\mathrm{t}}_{\mathrm{xx}}(\Delta\mathbf{r}) = I_0 \cos^2\theta \times \exp\{-4\pi^2(\sigma_{\mathrm{d}}/\lambda)^2(n_{\mathrm{x}}-1)^2[1-\exp(-\Delta\mathbf{r}^2/r_{\mathrm{d}}^2)]\}, \tag{6a}$$

$$W^{\mathrm{t}}_{\mathrm{yy}}(\Delta\mathbf{r}) = I_0 \sin^2\theta \times \exp\{-4\pi^2(\sigma_{\mathrm{d}}/\lambda)^2(n_{\mathrm{y}}-1)^2[1-\exp(-\Delta\mathbf{r}^2/r_{\mathrm{d}}^2)]\}, \tag{6b}$$

$$\begin{aligned} W^{\mathrm{t}}_{\mathrm{xy}}(\Delta\mathbf{r}) =& [W^{\mathrm{t}}_{\mathrm{yx}}(\Delta\mathbf{r})]^* = I_0 \sin\theta\cos\theta \exp\{\mathrm{j}2\pi\bar{d}(n_{\mathrm{x}}-n_{\mathrm{y}})/\lambda\} \\ & \times \exp\{-2\pi^2(\sigma_{\mathrm{d}}/\lambda)^2[(n_{\mathrm{x}}-1)^2+(n_{\mathrm{y}}-1)^2 \\ & -2(n_{\mathrm{x}}-1)(n_{\mathrm{y}}-1)\exp(-\Delta\mathbf{r}^2/r_{\mathrm{d}}^2)]\}. \end{aligned} \tag{6c}$$

When Equations 6a-6c have been derived, the surface of the polarization scattering spot is assumed to be rough and wide-sense stationary where its correlation function depends only on the differences of measurement coordinates: $\Delta\mathbf{r} = |\mathbf{r}_1 - \mathbf{r}_2|$. These results provide us with a specific relationship between the correlation properties of the transmitted electric fields and the micro-structure of the rough surface of the retardation plate.

To provide physical insight into these results, we have presented some numerical examples by taking the following parameters: $I_0 = 1$, $\theta = \pi/4$, $n_{\mathrm{x}} = 1.486$ and $n_{\mathrm{y}} = 1.658$ for the birefringent material: calcite [12]. Figure 2 illustrates the normalized correlation functions for each element in the coherence tensor: $\eta^{\mathrm{t}}_{lm}(\Delta\mathbf{r}) = W^{\mathrm{t}}_{lm}(\Delta\mathbf{r})/W^{\mathrm{t}}_{lm}(0)$ indicating the degree of coherence between l and m components of the field immediately behind the scattering surface at the surface for several values of σ_{d}. Note that the normalized correlation functions $\eta^{\mathrm{t}}_{lm}(\Delta\mathbf{r})$ are not influenced by the average thickness of the birefringent plate $\bar{d}$. For large separation $\Delta\mathbf{r}$, these normalized correlation functions approach their non-zero asymptotes, respectively. They are $\exp[-4\pi^2(n_{\mathrm{x}}-1)^2\sigma_{\mathrm{d}}^2/\lambda^2]$, $\exp[-4\pi^2(n_{\mathrm{y}}-1)^2\sigma_{\mathrm{d}}^2/\lambda^2]$ and $\exp\{-2\pi^2[(n_{\mathrm{x}}-1)^2+(n_{\mathrm{y}}-1)^2]\sigma_{\mathrm{d}}^2/\lambda^2\}$ with their values rapidly approaching zeros as σ_{d} grows. These asymptotes indicate that the transmitted electric field passing through the retardation plate has a non-negligible specular transmission of the incident light, as can be easily seen by noting the flat correlation functions when $\sigma_{\mathrm{d}} = 0$, in which only a specular transmission light exists. To study the non-specular component in the scattered light, it is helpful to subtract out these asymptotes of the correlation functions, yielding

$$'W^{\mathrm{t}}_{lm}(\Delta\mathbf{r}) = W^{\mathrm{t}}_{lm}(\Delta\mathbf{r}) - W^{\mathrm{t}}_{lm}(+\infty). \tag{7}$$

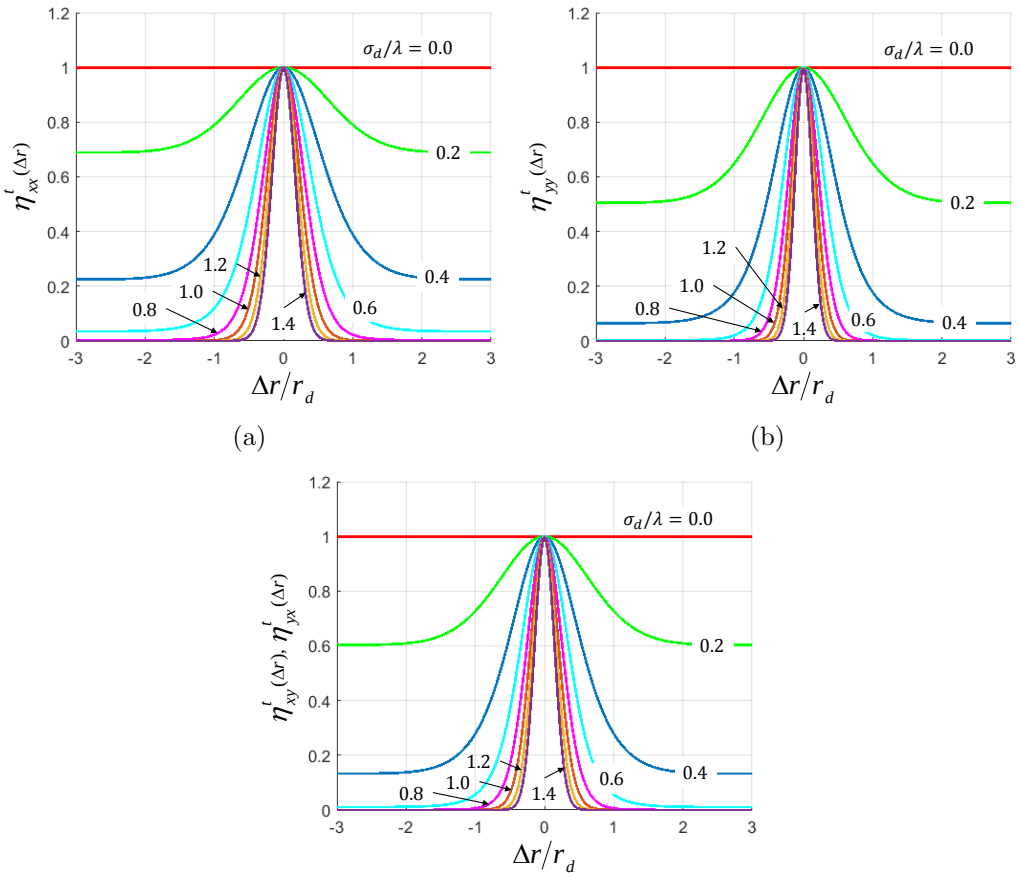

Figure 2: The normalized correlation functions of each component of the electric field vector describing the correlation properties of the scattered electrical field and the surface thickness fluctuations of the birefringent material.

The coherence area A_{c} of this non-specular component of the scattered electric field can be found by evaluating [6]

$$A_{\mathrm{c}} = 2\pi \int_0^{+\infty} \left(\mu^{\mathrm{t}}\right)^2 \Delta\mathbf{r}\, \mathrm{d}\Delta\mathbf{r}, \tag{8}$$

where $\left(\mu^{\mathrm{t}}\right)^2$ is the electromagnetic degree of coherence given by [13]

$$\left(\mu^{\mathrm{t}}\right)^2 = \frac{|'W^{\mathrm{t}}_{\mathrm{xx}}(\Delta r)|^2 + |'W^{\mathrm{t}}_{\mathrm{xy}}(\Delta r)|^2 + |'W^{\mathrm{t}}_{\mathrm{yx}}(\Delta r)|^2 + |'W^{\mathrm{t}}_{\mathrm{yy}}(\Delta r)|^2}{\left(|'W^{\mathrm{t}}_{\mathrm{xx}}(0)| + |'W^{\mathrm{t}}_{\mathrm{yy}}(0)|\right)^2}. \tag{9}$$

Figure 3 shows a plot of $\left(\mu^{\mathrm{t}}\right)^2$ when σ_{d} takes on several different values.

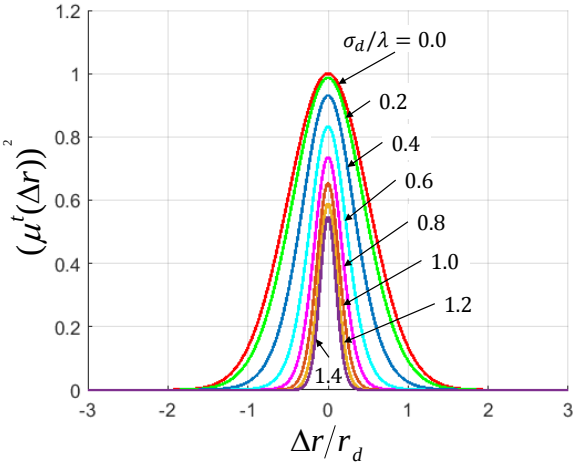

Figure 3: Distribution of $\left(\mu^{\mathrm{t}}\right)^2$ for various values of σ_{d}.

As σ_{d} increases, the area covered by the curve of $\left(\mu^{\mathrm{t}}\right)^2$ decreases. The coherence area A_{c} in Eq. 8 provides a useful measure of the average "size" of the scattered electric field. It can readily been seen that when only a specular transmission exists for a super smooth surface with $\sigma_{\mathrm{d}} = 0$, $\left(\mu^{\mathrm{t}}\right)^2$ for the transmitted electric field becomes singular and can be found by using L'Hôpital's rule, that is: $\lim_{\sigma_{\mathrm{d}}/\lambda \to 0} \left(\mu^{\mathrm{t}}\right)^2 = \mathrm{e}^{-2(\Delta\mathbf{r}/r_{\mathrm{d}})^2}$, and the corresponding surface thickness correlation area can be estimated as $A_{\mathrm{stc}} = 2\pi \int_0^{+\infty} \mathrm{e}^{-2(\Delta\mathbf{r}/r_{\mathrm{d}})^2} \Delta\mathbf{r}\, \mathrm{d}\Delta\mathbf{r} = \pi r_{\mathrm{d}}^2/2$. Figure 4 shows a plot of the transmitted field correlation area A_{c} normalized by the surface-thickness correlation area A_{stc} vs. the standard deviation of the rough surface fluctuation

normalized by the incident wavelength $\sigma_{\rm d}/\lambda$. Note that when the standard deviation of the rough-surface fluctuation reaches the wavelength of the incident wave, the correlation area of the scattered electric fields is about 1/20 of the surface-thickness correlation area. The reason for the shrinking of the correlation area for the scattered fields as the standard deviation of the surface roughness increases lies in the fact that when the surface thickness fluctuation for the retardation plate begin to exceed the incident wavelength, the phase difference between the $\hat{\rm x}$ and $\hat{\rm y}$ components of the electric fields is beyond 2π and the field transmitted by such rough-surfaced retardation plate will contain rays with all states of polarization. Clearly for large value of $\sigma_{\rm d}$, the correlation area of the scattered electric field is much smaller than the correlation area of the surface thickness itself.

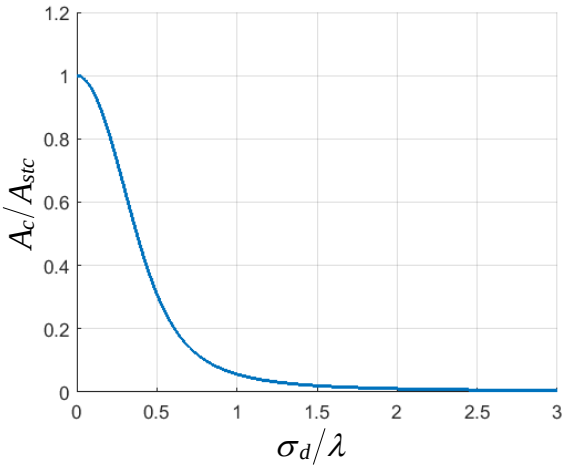

Figure 4: Normalized coherence area $A_{\rm c}/A_{\rm sct}$ of the scattered electric fields vs. the standard deviation of the surface thickness fluctuation scaled by the wavelength.

Another interest here is the random spatial distribution of the polarization state for the static scattered light. Monochromatic light with negligible temporal fluctuations, e.g. laser light, creates such a static random field called polarization speckle field. Despite its notable spatial disorder, the field is fully polarized at each point according to the traditional definition of the degree of polarization, which replaces the ensemble average with the time average and does not take into account the spatial randomness of the polarization speckle field. To specify the spatial statistical property for surface polarization scattering, we will use the spatial degree of polarization defined

by [14]

$$P(\mathbf{r}) = \left\{ 1 - \frac{4 \det \mathbf{W}(\mathbf{r}, \mathbf{r})}{[\mathrm{tr}\ \mathbf{W}(\mathbf{r}, \mathbf{r})]^2} \right\}^{1/2}, \tag{10}$$

where tr and det indicate the trace and determinant of the matrix, respectively; and the spatial average has been adopted for ensemble average when coherence matrix in Eq. 2 and Eqs. 6 have been estimated. On substituting from Eqs. 6a-6c into Eq. 10, we obtain the spatial degree of polarization for the scattered light immediately behind the depolarizer surface. That is $P^{\mathrm{t}} = \sqrt{1 - \sin^2(2\theta)\left[1 - \exp\left\{-4\pi^2(\sigma_{\mathrm{d}}/\lambda)^2(n_{\mathrm{x}} - n_{\mathrm{y}})^2\right\}\right]}$. Similar to the coherence analysis above, to study the stochastic polarization property for the non-specular component of the scattered light, the spatial degree of polarization can be also estimated by substituting Eq. 7 for $\Delta\mathbf{r} = 0$ into Eq. 10 when the asymptotes of the correlation functions for the element in the coherence matrix have been subtracted.

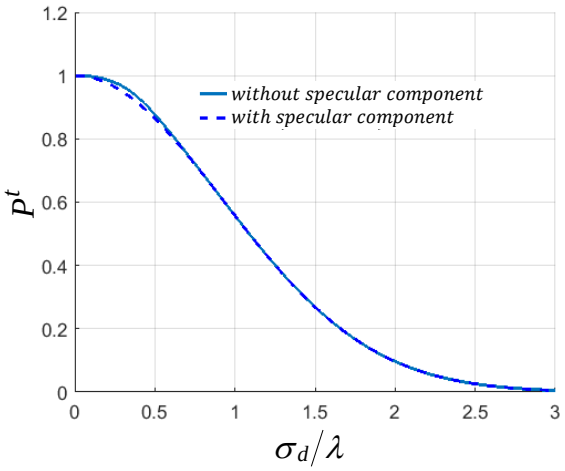

Figure 5: Spatial degree of polarization for surface polarization scattering as a function of $\sigma_{\mathrm{d}}/\lambda$.

Figure 5 shows the spatial degree of polarization P^{t} for the scattered electric fields with and without specular component vs. the standard deviation for the surface thickness fluctuation normalized by the wavelength. Basically, these two curves look similar except that P^{t} for the scattered light without specular transmission looks a little bit flat for small value of $\sigma_{\mathrm{d}}/\lambda$. As $\sigma_{\mathrm{d}}/\lambda$ grows large, the spatial degree of polarization reduces to zero monotonically. Note that when the surface-thickness standard deviation reaches beyond 2π,

the spatial degree of polarization for the scattered light at the surface is less than 1/10 indicating a depolarization effect to scramble the incident polarization. Therefore, the scattered electric field at the surface can be reasonably considered as a spatially unpolarized light. Such depolarization analysis on birefringent material will be of benefit to design and optimization of depolarizers used under different circumstances [16]. Comparing Figure 4 and Figure 5, we further note that the widths at half maximum of P^{t} is much broader than that of $A_{\mathrm{c}}/A_{\mathrm{sct}}$ indicating that the realization of depolarization is much more difficult than that of decoherence for the scattered light introduced by increasing the standard deviation of the rough-surfaced retardation plate.

In summary, we have explored the statistical properties for the scattered light at the surface of birefringent material. Subject to some simplifying assumption, we have studied the coherence and polarization properties for the surface polarization scattering and have found that these statistical properties depend in a complex way on both the surface-thickness variance and the lateral radius for the surface thickness correlation. In particular, we have shown that scrambling the incident polarization is much more difficult than reducing the coherence for the scattered light introduced by a rough surface of birefringent material. Further, a systematic analysis of statistical properties of scattered electric field depending on the micro-structure of the rough surface from birefringent material will be beneficial to understand the underlying mechanism of the surface scattering and therefore open up new opportunities of wide applications including optical manufacturing, biomedical imaging, and optical meteorology [17, 18].

Funding. Engineering and Physical Sciences Research Council (EPSRC) (EP/K03643/1); Scottish Universities Physics Alliance (SUPA) (SSG040); Japan Society for the Promotion of Science (JSPS) (25390090).

Acknowledgement. J. Ritter and N. Ma gratefully acknowledge their scholarship supports from Cusanuswerk (Germany) and Nelson Fund respectively to support their studies in UK.

[1] L. Tsang, J. A. Kong and K-H. Ding, Scattering of Electromagnetic Waves, Theories and Applications (Wiley, 2008).

[2] A. V. Osipov and S. A. Tretyakov, Modern Electromagnetic Scattering Theory with Applications (Wiley, 2017).

[3] C. C. Sung and J. A. Holzer, "Scattering of electromagnetic waves from a rough surface," Appl. Phys. Lett. 28, 429–431 (1976).

[4] J. A. Holzer and C. C. Sung, "Scattering of electromagnetic waves from a rough surface. II," Journal of Applied Physics 49, 1002–1011 (1978).

[5] N. Ma, S. G. Hanson, M. Takeda and W. Wang, "Coherence and polarization of polarization speckle generated by a rough-surfaced retardation plate depolarizer," J. Opt. Soc. Am. A 32, 2346–2352 (2015).

[6] L. Mandel and E. Wolf, Optical Coherence and Quantum Optics (Cambridge University, 1995).

[7] E. Wolf, Introduction to the Theory of Coherence and Polarization of Light (Cambridge University Press, 2007).

[8] F. Gori, M. Santarsiero, S. Vicalvi, R. Borghi, G. Guattari et al., "Beam coherence-polarization matrix," Pure and Applied Optics: Journal of the European Optical Society Part A, vol. 7, no. 5, 941 (1998).

[9] J. W. Goodman, Statistical Optics (Wiley, 2000).

[10] J. C. Dainty, Laser Speckle and Related Phenomena (Springer, 1984).

[11] J. W. Goodman, Speckle Phenomena in Optics: Theory and Applications (Roberts & Company, 2007).

[12] E. Hecht, Optics (Addison-Wesley, 2015).

[13] J. Tervo, T. Setala and A. T. Friberg, Opt. Express 11, 1137 (2003).

[14] W. Wang, S. G. Hanson, and M. Takeda, "Statistics of polarization speckle: theory versus experiment," Proc. SPIE 7388, Ninth International Conference on Correlation Optics, 738803 (2009).

[15] G. Basso, L. Oliveira and I. Vidal, "Complete characterization of partially coherent and partially polarized optical fields," Optics Letters, vol. 39, 12201222 (2014).

[16] C. J. Peters, "Light Depolarizer," Appl. Opt. 3, 1502–1503 (1964).

[17] L. Liu, X. Li, and K. Nonaka, "Light depolarization in off-specular reflection on submicro rough metal surfaces with imperfectly random roughness," Rev. Sci. Instrum. 86, 023107 (2015).

[18] L. Liu and K. Nonaka, "Beam diameter thresholds as applying light depolarization for effective submicron and micron root mean square roughness evaluation," Appl. Opt. 56, 7024–7032 (2017).